THE UNIVERSITY OF MICHIGAN RESEARCH INSTITUTE
ANN ARBOR, MICHIGAN

Progress Report

SULFIDE INCLUSIONS IN STEEL

L. H. Van Vlack
O. K. Riegger
R. J. Warrick

UMRI Project 2703

U.S. STEEL CORPORATION
PITTSBURGH, PENNSYLVANIA

August 1958

ABSTRACT

The shape and distribution of sulfide inclusions in iron and steel were investigated. Particular emphasis was placed on (1) the effects of oxygen, carbon, silicon, and manganese, and (2) the effect of temperature.

Work was performed on metals ranging from pure iron to compositions nearly identical to B-1113 and rimming steels. The technique which was used involved microscopic observations of structures arising from heat treatments in the rolling temperature ranges. Ingot solidification and pre-rolling microstructures could be simulated.

The principal findings are the following. (1) Oxygen globularizes liquid sulfide inclusions along the austenite grain boundaries. (2) Silicon and carbon, as such, have no major effect upon the sulfide distribution in iron-sulfur alloys. (3) When both oxygen and silicon are present in quantities encountered in resulfurized steels, silicon will deoxidize the sulfide inclusions and remove the effect of oxygen in (1) above. (4) Manganese affects the sulfide inclusions in steel more markedly than previously supposed. This will necessitate some modification of the present theory of the mechanism of hot-shortness.

Further work should include (1) a determination of the solubility of oxygen, silicon, and metallic elements in liquid and solid (Fe,Mn)S, and (2) a more detailed investigation of the role of manganese on the intergranular distribution of sulfides on steel. Each approach would be related to hot-shortness and to resulfurized steel.

INTRODUCTION

Sulfide inclusions are undesirable in most steels because they contribute to hot-shortness. However, their presence in free-machining steels is intentional. In each case, the size and distribution of the sulfides within the austenite matrix is important. Hot-shortness is commonly explained on the basis of a liquid sulfide film between the iron grains.[1] Supposedly, this film provides a surface of weakness within the steel along which ruptures start. Machinability is also related to the size and distribution of inclusions in rolled steels.[2] Without doubt, the geometric variation in rolled products is related to size, shape, and composition of the inclusions solidifying from the molten steel.

This study has been concerned with the effect of compositional variations upon the geometric characteristics of sulfide inclusions in metals ranging from pure iron to those nearly identical with B-1113 and rimming steels. This work is closely related to concurrent studies by Silverman and Snow[3] on the phase relationships in manganese sulfide-silicate and manganese sulfide-oxide melts. Close technical contact was maintained with their work during the progress of the investigation.

EXPERIMENTAL WORK

The experimental work involved three steps: (1) the melting of samples, (2) heat treatments to simulate as-cast or soaking pit conditions, and (3) microscopic examination of the geometric variables. Each step underwent some modification for experimental improvement during the course of the investigation. The most satisfactory procedure is described briefly here. Appendix B gives a more detailed description for possible future reference.

(1) SAMPLE MELTING

The metal compositions were prepared with 1/2-in. Ferrovac rod as the source of relatively pure iron. Reagent grade sulfur and Fe_2O_3, 90% ferrosilicon, low-ash carbon electrode, and electrolytic manganese were used as additions to synthesize the required compositions. The desired quantity of sulfur, oxygen, and silicon were placed in a cavity within a Ferrovac rod. The rod, plus carbon and manganese additions, were heated by an induction coil in a mechanical vacuum until melting occurred.

Recrystallized Al_2O_3 and alundum thimbles were used as crucible materials. Heating was extended for only about 1/2 minute beyond complete melting to minimize any possible reaction between the melt and the crucible. The sample solidified within about a minute after the power was shut off. Segregation was nil.

(2) HEAT TREATMENTS

The samples for heat treatments were diametric cross sections of the solidified melt. An average thickness of only 1/8 in. assured the maximum quenching rate after heat treatment.

The temperatures for heat treatment were in the soaking and rolling ranges. An exact duplication of steel-mill temperature sequences was not made because a concurrent duplication of rolling forces could not be incorporated. However, the equilibrium microstructures were readily obtained within the production temperature range by appropriate heating times (Table I). The normal temperature drop in production would represent a time-wise integration of these structures.

TABLE I. HEAT-TREATMENT SCHEDULES

Temperature, °F	Time, hr	
	Liquid Sulfides	Solid Sulfides
2600	-	2
2400	1/2	16
2300	1	-
2100	2	36
1900	2	-
1750	4	85

Two procedures were used during heat-treating. The first involved the use of an inert atmosphere (helium or nitrogen) deoxidized over hot calcium chips (1200°F). This procedure permitted sub-second quenching and was very desirable for cooling from those temperatures at which considerable iron was dissolved into the sulfide liquid. The second procedure involved heat-treating in a small, evacuated fused-silica tube. The tube could be mechanically broken during the quench to help accelerate the temperature drop. This evacuated-tube procedure provided a minimum of oxygen contamination for those compositions requiring long heat treatments.

(3) MICROSCOPIC EXAMINATION

Standard procedures for metallographic preparation were used. The microscopic distribution of the sulfide inclusions was evaluated according to the techniques of Smith[4] which make use of relative interfacial energies. Modifications of data representation were made to index more readily the relative energies. These modifications involved cumulative curves of dihedral angle probabilities (see Appendix A). The significant figures of such curves are the values of median angles, since they may be used as a direct index of the shape and distribution of inclusions between austenite grains (Fig. 1).

RESULTS AND DISCUSSION

This initial work and the results involved simple mixtures of (1) iron and sulfur, followed by (2) iron, silicon, and sulfur, (2) iron, oxygen, and sulfur, (4) iron, silicon, oxygen, and sulfur, (5) iron, carbon and sulfur, and (6) iron, carbon, manganese, and sulfur. These provided a progressive sequence from simpler compositions which had already been surveyed qualitatively[5,6] to those compositions which approximated commercial steels.

(1) IRON AND SULFUR (Figs. 1a and 2)

Above 2000°F, the sulfide forms a liquid phase. Because the inclusion angles are less than 30°, they have a rather extensive, but not a complete intergranular distribution (Fig. 1a). Figure 2 shows that a negligible temperature effect exists. This is in contrast to earlier qualitative work[8] in which the angle apparently dropped to zero around 2350°F. However, the earlier work did not involve complete sample melting. This work indicates that the temperature for a 0° angle is in excess of 2400°F.

A marked change in distribution occurs below the eutectic temperature where the sulfide inclusions were solid. This is consistent with former observations.

(2) IRON, SILICON, AND SULFUR (Fig. 3)

At steel-rolling temperatures, 2300°F, the measured penetration angles of the sulfides between the austenite grains were within a 5° range (24°-29°) when the silicon content varied from 0 to 0.1%. Since variations of less than 5° cannot be considered significant unless they are part of a general trend, it may be concluded that the distribution of inclusions in free-machining steels cannot be a function of silicon alone. (Later, it will be noted that silicon has an effect when oxygen is present.)

The silicon levels in these steels were not carried to higher values. Thus no conclusion can be made here about the effect of silicon on sulfides in a killed steel. However, previous qualitative work using 1% silicon suggested no significant effects arise.[7]

(3) IRON, OXYGEN, AND SULFUR (Figs. 1 and 4)

Oxygen tends to globularize sulfide inclusions between austenite grains.

This rather marked effect is in agreement with earlier qualitative data.[8] The addition of a few points (0.03%) of oxygen reduces the film formation by doubling the inclusion angle between the austenite grains. As a result, subsequent rolling would be less likely to produce numerous small inclusions than would an oxygen-free metal.

(4) IRON, SILICON, OXYGEN, AND SULFUR (Fig. 5)

In the absence of silicon, a 0.03% oxygen addition to iron-sulfur mixtures had a significant effect upon the inclusion shape and distribution. When 0.03% silicon was also present, the previous effect was not apparent. Furthermore, when excess oxygen (0.3%) was added, the modifying effect of the small amount of silicon was exceeded.

The most plausible explanation for the above observation is that the silicon deoxidizes the liquid sulfide phase when approximately 0.03% (steel levels) of both oxygen and silicon are present.

(5) IRON, CARBON, AND SULFUR (Figs. 6, 7, and 8)

Carbon, over the range of 0.03 to 0.6%, has no demonstrable effect upon the inclusion distribution at 2300°F when the sulfur content is held constant at 0.3% (Fig. 6).

However, a noticeable effect was observed when both carbon and sulfur were varied together at 2300-2400°F. Increased additions of equal amounts of carbon and sulfur produced more liquid. The additional liquid did not form a grain-boundary film at 2300°F. It did at 2400°F (Figs. 7 and 8). This effect cannot be satisfactorily explained at the present. Any speculation would have to involve variations in the carbon, iron, and sulfur composition of the liquid phase.

These observations cannot be directly related to the difficulties encountered in rolling resulfurized steels with greater than 0.12% carbon. More probably, those difficulties are related to the effect of carbon on delta-ferrite.

(6) IRON, MANGANESE, CARBON, AND SULFUR—B-1113 (Figs. 9 and 10)

The predominant effect of manganese additions is the production of solid sulfides at steel-rolling temperatures. This effect, which produces equiaxed sulfide inclusions, was expected. Unexpected was the fact that the required amount of manganese was very low. Only 0.15% manganese raised solidification temperature of the sulfides above 2400°F (but below 2600°F). At steel-rolling temperatures an intergranular film is absent.

The melting temperature of the sulfide phase in metal containing 0.1% C, 0.9% Mn, and 0.3% S is above 2600°F. This composition is nominal for B-1113 steel. Missing, however, are unspecified amounts of oxygen and silicon which usually fall in the range of 0.03%.

RESULFURIZED STEELS

Several hypotheses may be advanced to account for silicon's effect upon increasing the number and decreasing the size of the sulfide inclusions.[2] (1) Silicon dissolves in, and changes the characteristics of the sulfide phase. (2) Oxygen dissolves in the sulfide phase, if it is not removed by silicon. In turn the oxygen produces a more globular sulfide. (3) Silicon produces silicates which flux the sulfides (Silverman and Snow).[3]

Of these three, the first is considered unlikely but has never been experimentally excluded. It is proposed that an effort be made to determine the solubility (or lack of solubility) of silicon in solid and liquid sulfides.

The second suggestion is consistent with the results of this study. More should be known about the oxygen solubility in (Fe,Mn)S. Furthermore, steels with varying oxygen levels, and therefore differences in sulfide shape and distribution, should be rolled to correlate pre-rolling and rolled inclusions.

The last possibility is interesting since work at the Applied Research Laboratory has shown that MnS can be fluxed by silica and orthosilicates. However, FeS is not fluxed by silica,[9] and it is not known how intermediate (Fe, Mn)S will react.

HOT-SHORTNESS

A paradox has existed inasmuch as sulfur produces hot-shortness in steels. At the same time, resulfurized steel with 0.10 to 0.30% or more of sulfur may be rolled quite satisfactorily. The general explanation for hot-shortness is that a liquid sulfide film is formed around the austenite grains at steel-rolling temperatures. In most steels, a Mn/S ratio of 20 to 1 or 30 to 1 is required to "produce a solid sulfide." In resulfurized steels, the Mn/S ratio may be as low as 3/1 with no hot-shortness. The results of this study indicate that as little as 0.15% manganese removes the tendency for grain-boundary sulfide films at 2400°F.

The present progress of the work on sulfide inclusions cannot account for these apparent discrepancies. The only possible explanation at the present is based on the possibility that the sulfide inclusions in rimmed and killed steels are fluxed by small amounts of siliceous impurities. Additional work should be done to determine the microdistribution of sulfides when silica and other oxides are also present.

SUMMARY

Although this report covers only an inital period of work on sulfide inclusions in steels, certain findings may be summarized. These include: (1) Oxygen globularizes liquid sulfide inclusions along the austenite grain boundaries. (2) Silicon and carbon, as such, have no major effect upon the sulfide distribution in iron-sulfur alloys. (3) When both oxygen and silicon are present in quantities encountered in resulfurized steels, silicon will deoxidize the sulfide inclusions and remove the effect of oxygen in (1) above. (4) The effect of manganese on the sulfide inclusions in steel is more marked than previously supposed. This will necessitate some modification of the present theory of the mechanism of hot-shortness.

RECOMMENDATIONS FOR FUTURE WORK

Recommendations for future work fall into three categories:

1. Additional work similar to that covered by this report on steels of B-1113 composition and rimming composition, but with further oxygen and silicon additions. The purpose would be to determine the effect of the fluxing action of silicates upon the size and distribution of inclusions in steel prior to rolling.

2. Determination of the solubility (if any) of silicon in liquid and solid iron-manganese sulfide. The purpose would be to check the possibility that silicon directly affects the properties of iron-manganese sulfides.

3. Determination of the solubility of oxygen in liquid and solid iron-manganese sulfides. The purpose would be to explore more specifically the mechanism of the oxygen influence upon the shape and distribution of sulfide inclusion between austenite grains.

This work would supplement, but not overlap, the present work of the Applied Research Laboratory, in which detailed phase relationships are being studied in the MnS-Fe_2SiO_4-Mn_2SiO_4 and the MnS-FeO-MnO systems, nor would it conflict with possible future extension of that work into the MnS-metasilicate system.[10]

Long-range planning should include the rolling of steels with known high-temperature microstructures so that the effects of deformation upon inclusion may be studied.

ACKNOWLEDGMENTS

During the course of the work there were a number of meetings with personnel of the U. S. Steel Corporation: G. Eusner, J. Gambill, T. Garvey, A. Keh, G. Silverman, R. Snow, and H. Tata, each of whom made significant contribution to the plans and helpful criticisms of the interpretation of this investigation.

The suggestions and help of R. Wells of The University of Michigan are also acknowledged.

REFERENCES

1. "Hot-Shortness," Metals Handbook, American Society for Metals, Cleveland, p. 451.

2. Van Vlack, L. H., "Correlation of Machinability with Inclusion Characteristics in Resulfurized Bessemer Steels," Transactions of ASM, 45, 741-757 (1953).

3. Silverman, G., and Snow, R., United States Steel Corporation, Applied Research Laboratory, unpublished.

4. Smith, C. S., "Grains, Phases and Interfaces; An Interpretation of Microstructure," Transactions AIME, 175, 15-51 (1948).

5. Van Vlack, L. H., Interfacial Energies of Some Metallic Non-Metallic Systems and Their Relation to Microstructure, The University of Chicago, 1950.

6. Keh, A. S., and Van Vlack, L. H., "Microstructure of Iron Sulfur Alloys," Journal of Metals, 950-958 (1956).

7. Keh, A. S., Distribution of Sulfide Inclusions in Iron, The University of Michigan, Ann Arbor, 1955.

8. Van Vlack, L. H., "Intergranular Energy of Iron and Some Iron Alloys," Transactions AIME, 191, 251-259 (1951).

9. Riegger, O., unpublished.

10. Silverman, G., verbal communication.

APPENDIXES

APPENDIX A

SHAPE AND DISTRIBUTION MEASUREMENTS

The equilibrium size, shape, and distribution of a minor phase within a metal depends to a large extent upon the energies of the related interfaces. Thus, if the energy of the liquid phase boundary (e.g., sulfides in steel at high temperatures) is less than one-half of the grain-boundary energy of the solid phase, it is 'cheaper' energy-wise to form two liquid/solid interfaces than one solid/solid interface (i.e., the grain boundary). As such, a minor phase can form a complete network around the grains of the major phase (Fig. 11a). The minor phase would be widely distributed throughout the metal in this case.

In contrast, if the energy of the two-phase interface is greater than one-half of the grain-boundary energy, a complete intergranular film of the minor phase will not form. The result will produce a phase with angles which depend upon the relative interfacial energies. This is illustrated in Fig. 11b where the angle is such that the vectors of the energies are balanced. If the angle is greater than 60°, the minor phase is found only at the corners between four grains. Consequently, it is always equiaxed, or 'globular' (Fig. 11c). If the angle is 60°, the minor phase will distribute itself along the edges between three adjacent grains. The amount of solid-to-solid contact is still quite large. As the angles decrease to less than 60°, they progressively promote a greater penetration of the minor phase along the grain boundaries of the major phase (Fig. 1).

The inclusion angles are thus an indication of the inclusions' micro-distribution. When the angles are large, 'globular' inclusions develop. When the angles are small, film-like inclusions develop. Since the microscope views only a 2-dimensional cut of a 3-dimensional structure, the true angles are seldom seen. However, it may be shown that the true angle is very close (within 1°) to the median angle of a statistical sample. Therefore, for purposes of indexing the shape of the inclusions, it is necessary only to measure a number of random angles and calculate their median. The number to be measured should be large enough so that the variance of the median is less than the variance for measuring individual angles. The latter differs somewhat from sample to sample but generally is in the range of $\pm$ 2°. This means that only about 25 angles are normally required for a statistical sample, and the microscopic analysis is considerably simpler than previously practiced.[4,8]

The data are handled best with a cumulative plot as shown in Fig. 12. Such a plot permits a quick visual determination of the median angle. Fur-

thermore, it shows at a glance whether the sample has developed geometric equilibrium (Fig. 12b). Neither of these facts is readily evident in the normal noncumulative frequency plots which have generally been used.

APPENDIX B

EXPERIMENT EQUIPMENT AND PROCEDURE

A. SAMPLE MELTING

Two melting furnaces were used during the course of this investigation: (1) a large laboratory vacuum-induction furnace and (2) a small external coil-induction furnace. Although all the reported results are based on heats melted in the latter furnace, the work involving the larger laboratory vacuum-induction furnace will be described for the record.

The larger furnace is capable of melting 5-lb heats in a vacuum of 5μ or better. The melting procedure involved (1) charging 3 or more pounds of Armco iron into a zirconia crucible, (2) evacuating the furnace, (3) melting the iron, (4) adding the alloying elements to the molten metal at approximately 3100°F, (5) superheating to 3200°F, (6) casting into a steel mold 1-1/2 in. in diameter, and (7) allowing the ignot to cool for approximately 20 minutes. In each case the furnace pressure increased significantly during the addition of the alloying elements, and the cast structures were quite porous. Further, there were high losses of the alloy additions, particularly manganese and carbon. These results are attributable to the high initial oxygen content of the Armco iron. Inasmuch as the oxygen content proved to be significant during the study of the inclusions and the oxygen content of this source of iron was variable it is considered necessary to switch to a low-oxygen iron as a source material. Ferrovac "E" rod (Table II), which has a maximum oxygen content of 0.0076%, was used as a primary source of iron for all further melts. This change favored the use of a smaller melting crucible and the switch to the external coil-induction furnace. This led to (1) better control of the alloy content, (2) easier control of the ingot solidification rate when necessary, and (3) samples which were more readily handled for microscopic observation.

TABLE II. FERROVAC "E" ANALYSES

Element	Lot 1, % (3/8-in. rod)	Lot 2, % (1/2-in. rod)
C	0.025	0.008
Mn	0.001/0.005	< 0.01
Si	0.007	< 0.01
O	0.0023	0.0076
N	0.0004	0.0004
P,S,Mo,Cr,V,Sn,Al,Co,Cu,Pb	< 0.01	< 0.01
Ni	0.005	0.04

The smaller, external coil vacuum-induction furnace which was built is shown in Fig. 13. It had a 2-3/8-in.-ID, water-cooled, copper induction coil which was approximately 6 in. high. A 50-by-400-mm pyrex glass tube was used as the outside shell and fit inside of the induction coil. Provision was made for the inlet of nitrogen, helium, or argon and an exhaust to a mechanical vacuum pump. A mercury manometer was attached for general vacuum measurements.

Two types of arrangements were used to center the crucibles and to protect and to insulate the pyrex shell. The first, shown in Fig. 13a, utilized a fused alumina sleeve mounted on an insulation brick pedestal and separated from the test tube by fiberfrax packing. The crucibles, 19-by-90-mm alundum thimbles, were placed inside a larger alundum thimble, which was a safeguard to prevent furnace damage in case the inner thimble was cracked during heating.

The second arrangement, shown in Fig. 13b, utilized an insulating brick. Both 19-by-90-mm alundum thimbles and 25-by-40-mm recrystallized alumina crucibles were used in this latter arrangement. This scheme proved to be more desirable since it combined greater simplicity and better operation. The first furnace arrangement was used for those melts in the iron-sulfur, iron-silicon-sulfur, and iron-carbon sulfur systems. The second arrangement with the alundum thimbles was used for iron-carbon-manganese-sulfur and iron-manganese-sulful melts. Recrystallized alumina thimbles were substituted for the iron-oxygen-sulfur and iron-silicon-oxygen-sulfur systems because they were less subject to attack by the oxygen-containing melts. Furthermore, they reduced the possibility of silica pickup during melting.

The vacuum system was capable of maintaining a furnace pressure of less than 1/2 mm of mercury throughout the melting cycle. This situation, coupled with the fact that the furnace was flushed and evacuated three times prior to melting with inert gas, provided a minimum of oxygen contamination.

The following materials were used as alloy additions: reagent grade sulfur and Fe_2O_3, 90% ferro-silicon, low-ash carbon electrode, and electrolytic manganese (99.99%). Sulfur additions were made in the form of FeS which had been previously prepared by reacting sulfur with a stoichiometric amount of Ferrovac "E" chips in an evacuated sealed pyrex tube at 850°F. The reaction was complete after 72 hours.

Ferrovac "E" rod was used as the source of high-purity iron. With the alundum thimbles, 1/2-in.-diameter rod was used, and with the recrystallized alumina thimbles, 3/8-in.-diameter rod. These choices were governed by the crucible geometry and provided for the most rapid melting. Holes approximately 1/8 in. less in diameter than the rod diameter were drilled to a depth of about 5/8 in. in the top of the rod. All the alloy additions with the exception of carbon and approximately one-half of the total manganese were placed in this cavity prior to melting. The latter were placed in the bottom of the crucible.

A typical melting cycle for nonoxygen-bearing melts would be as follows: (1) evacuate and flush the complete system three times, (2) continue evacuation

for approximately 20 minutes, (3) turn power one-half way up for one minute, (4) boost to full power, (5) shut off vacuum pump when the sulfide starts to melt (approximately 2-1/2 minutes after full power) and maintain the furnace pressure at approximately 15 mm of mercury by cycling the pump, (6) superheat at full power for from 30 to 45 seconds after the completion of the melt, (7) shut off power and let the ingot cool until solidified, (8) turn on the vacuum pump until the ingot is cold. Steps (3) through (6) took between 4 and 5 minutes.

With managanese-bearing melts this process was modified by extending the melting period for about 45 seconds at one-half power to insure complete solution and mixing of the MnS which was formed.

The oxygen-bearing heats were melted under an atmosphere of either purified argon or helium rather than a vacuum. The furnace was evacuated and flushed twice with an inert gas, and then refilled with a continuous gas stream until the ingot had cooled below red heat.

B. HEAT-TREATING EQUIPMENT AND PROCEDURES

The small ingots were cut into transverse slugs approximately 1/8 in. thick. The two end cuts were mounted to check the cast structure and for possible alloy segregation. The center cuts were used for succeeding heat treatments. Each ingot provided approximately eight samples.

The principal furnace used for heat-treating was a Leco globar furnace. Zircotubes were used to enclose the selected atmosphere. Thermocouples placed within these tubes adjacent to the samples indicated a maximum temperature variation of $\pm$ 10°F.

Two methods were used to maintain a neutral heat-treating atmosphere. The first involved the passing of inert gas such as nitrogen through a purifying train involving a desiccant and a deoxidizer. Of the several common possibilities, anhydrous $CaSO_4$ and calcium chips at 1200°F proved most satisfactory. The purified gas was continuously passed through the furnace at slightly above atmospheric pressure until the treatment was completed. At that time the furnace was opened up and the samples were quickly quenched in water. A long initial gas purge was used, and the exposure to the ambient atmosphere prior to quenching was a matter of seconds.

The second method for heat-treating involved sealing the specimens in a glass tube which had been evacuated. This technique was found to be especially advantageous where heat-treating times were long with the resulting increased possibility for oxygen contamination. At lower temperatures (i.e., 1750°F), an evacuated vycor tube was found to give satisfactory results. Above 2100°F a fused silica tube was used. The procedure followed was: (1) initial evacuation of the tube by a mechanical vacuum system, (2) bleeding in an inert atmosphere, usually nitrogen, and (3) repeating (1) and (2) several times before sealing with a selected amount of inert atmosphere. Usually 130 to 150 mm of

pressure was sealed in, but this varied with the anticipated heat-treating temperature so that the internal and external pressures were balanced. After heat-treating, a slight modification of the procedure was required; it was necessary to break the glass tube mechanically as it was quenched to provide a rapid quenching action. It is estimated that the total quenching time was in the order of from 2 to 3 seconds. The technique of heat-treating in a sealed tube under inert atmosphere offered two distinct advantages: heat treatments up to temperatures of 2700°F were possible, and sulfur volatilization was minimized.

C. METALLOGRAPHIC PREPARATION AND EXAMINATION OF SPECIMENS

All specimens were prepared for microscopic examination using standard metallographic techniques. The specimens were mounted and rough-polished on wet silicon carbide papers using 80, 400, and 600 grit papers. Final polishing was done by hand using 1-μ diamond paste on a standard polishing cloth. For photographic work, it was found necessary to remove the fine diamond scratches in the ferrite by using a few turns on a Linde-B wheel. Etchants were used only for the checking of the carbon contents.

Early examination of the cross sections of several of the heat-treated specimens showed the presence of two surface phenomena: surface oxidation due to water quenching, and sulfur depletion which never exceeded a maximum depth of 0.015 in. From 0.030 to 0.035 in. was ground off the surface of all heat-treated specimens to eliminate the effects of either type of surface phenomena on the microstructure to be observed. Approximately 0.015 in. was ground off the surface of the as-cast specimens where neither of the two previously mentioned types of surface phenomena could occur.

The untreated top and bottom cuts of all ingots were examined microscopically as a qualitative check on the melting procedure. In particular, attention was paid to the type and distribution of sulfides and the possible presence of any contaminants such as oxygen and silica. All heats except one showed evidence of thorough mixing and a reasonable lack of any contaminants. A few silicates were present in all heats and their general source appears to be the Ferrovac "E" rod. They were assumed not to be detrimental in the minute quantities which occurred.

All heat-treated specimens were examined microscopically as a qualitative examination of the heat-treating procedure and to obtain a general idea of the occurring trends in the type and distribution of the sulfides. As a result of these examinations, necessary heat-treatment modifications were made as noted in the previous section. All specimens which were improperly quenched, slightly contaminated with oxygen, or otherwise impaired were discarded at this point and the heat treatments rerun.

Quantitative angle measurements were made on selected samples with a Bausch and Lomb binocular metallograph possessing a rotating calibrated state and a

Filer eyepiece. The angle measurements were made using oil immersion lenses and magnifications of either approximately 1000X or 2000X. The angle size was determined by observing the number of degrees of stage rotation from a position tangent to one side of the sulfide inclusion vertex to a position tangent to the other side. Randomness was obtained by moving the stage laterally without looking at the structure, and then measuring the sulfide which was nearest the cross-hair. Only sulfides which showed definite interfacial angles were measured. Individual angle measurements were found to be reproducible to within about $\pm 2°$. The error of measurement increased slightly as the sulfide size decreased and as the angle size increased.

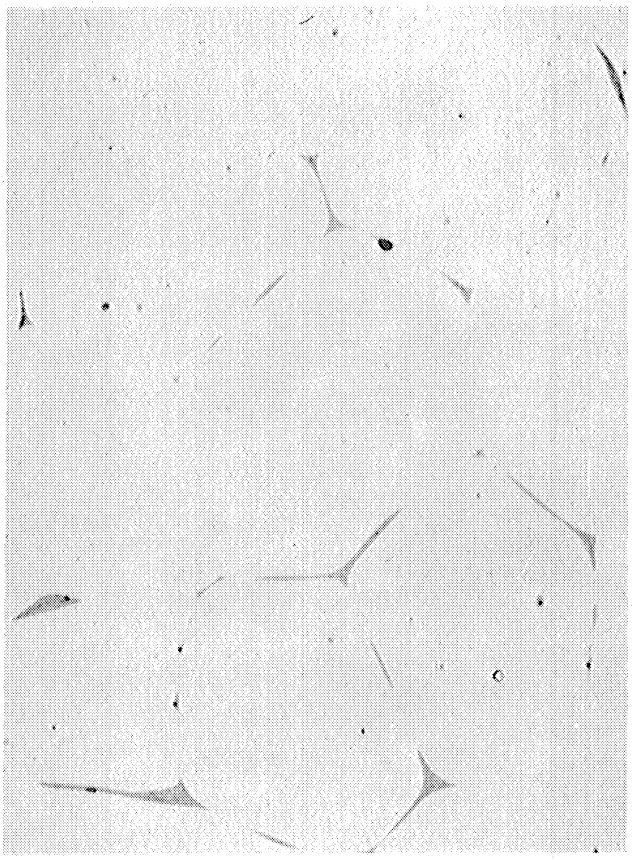

(a) No oxygen added (inclusion angle - 20°).

(b) 0.03% oxygen added (inclusion angle - 37°).

(c) 0.3% oxygen added (inclusion angle - 54°).

Fig. 1. Effect of oxygen. Oxygen changed the size and shape of sulfide inclusions at 2400°F (0.3% sulfur). X250.

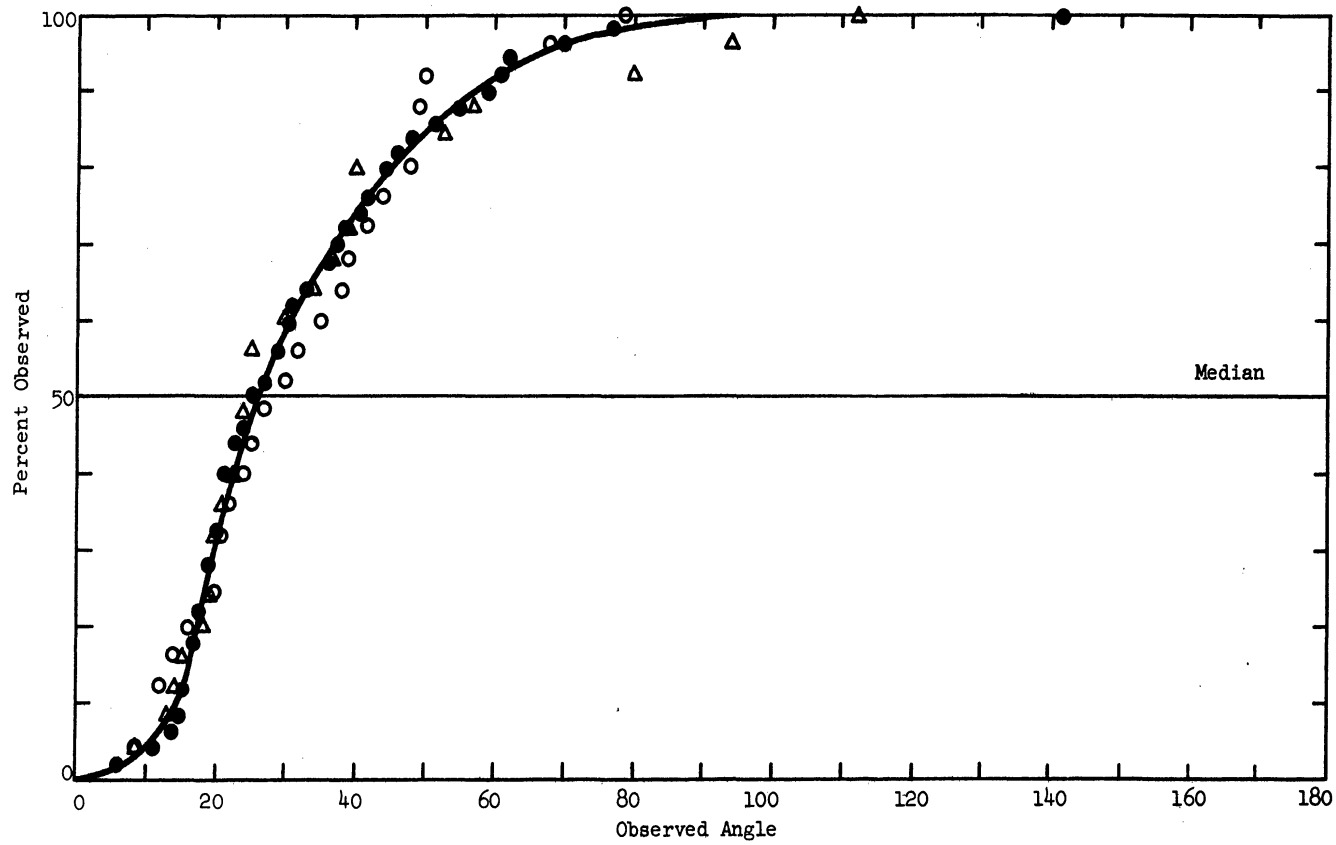

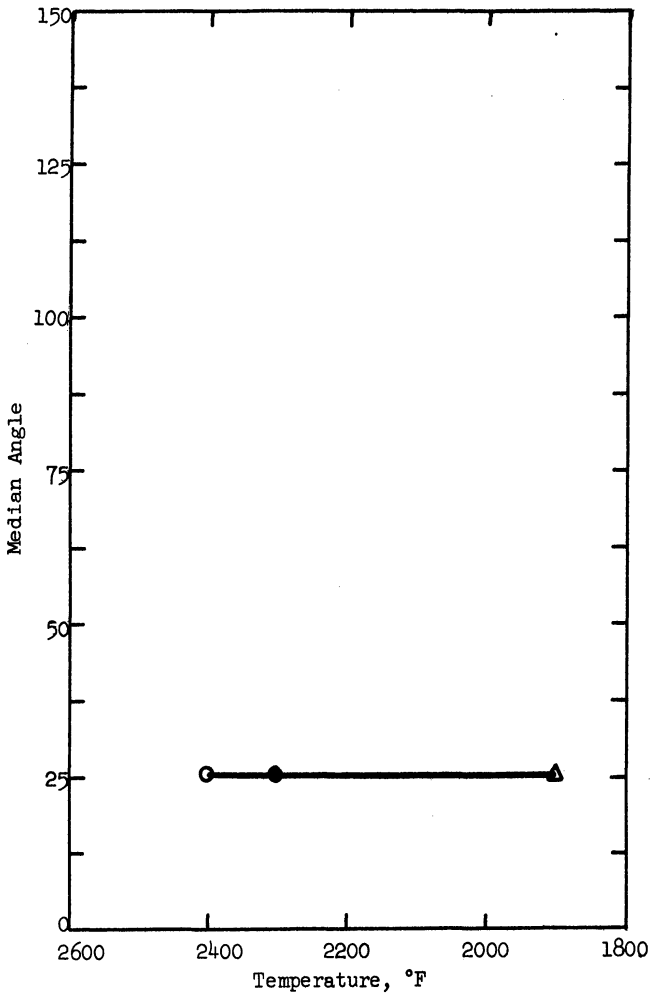

Symbol	Aim Composition, % S	Temperature, °F
○	0.30	2400
●	0.30	2300
△	0.30	1900

Fig. 2. Effect of temperature.

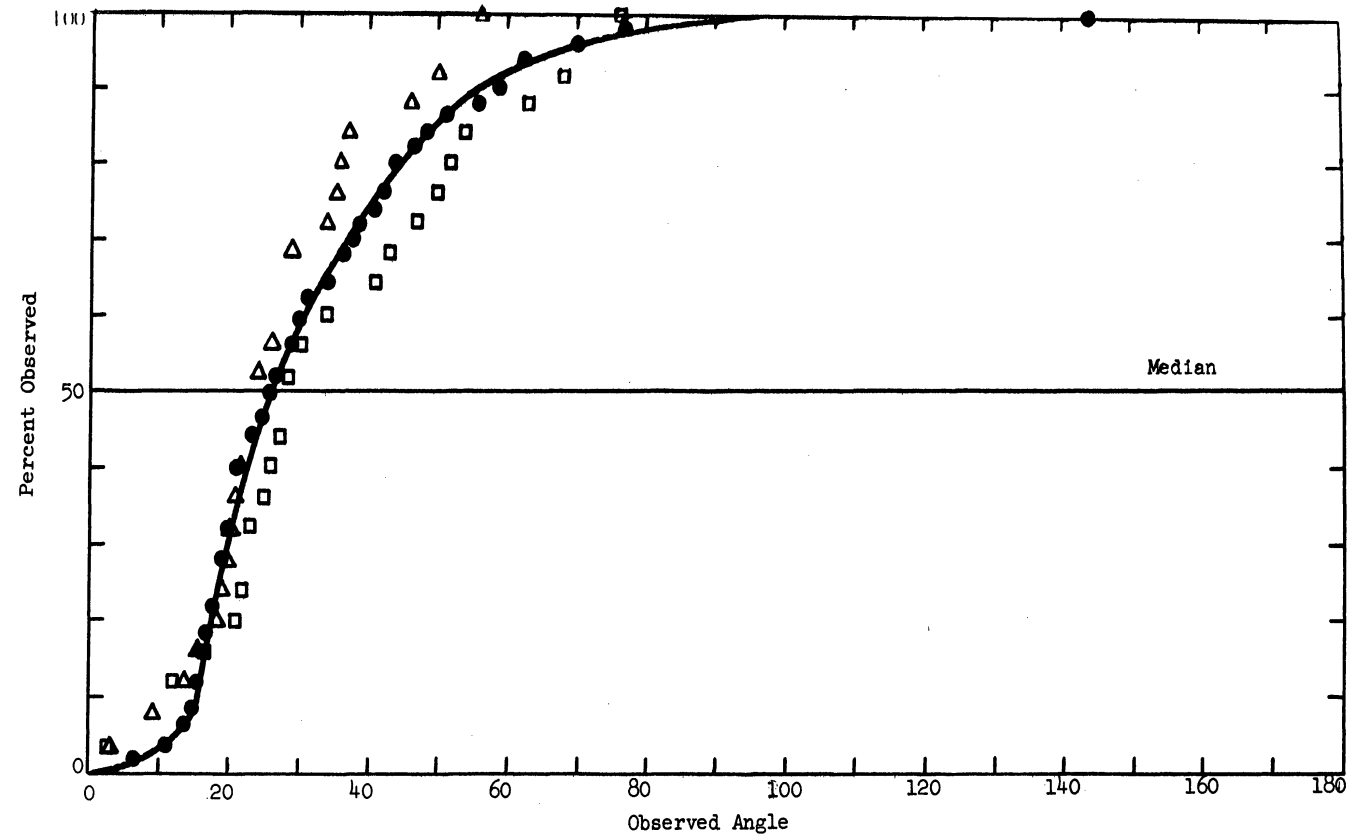

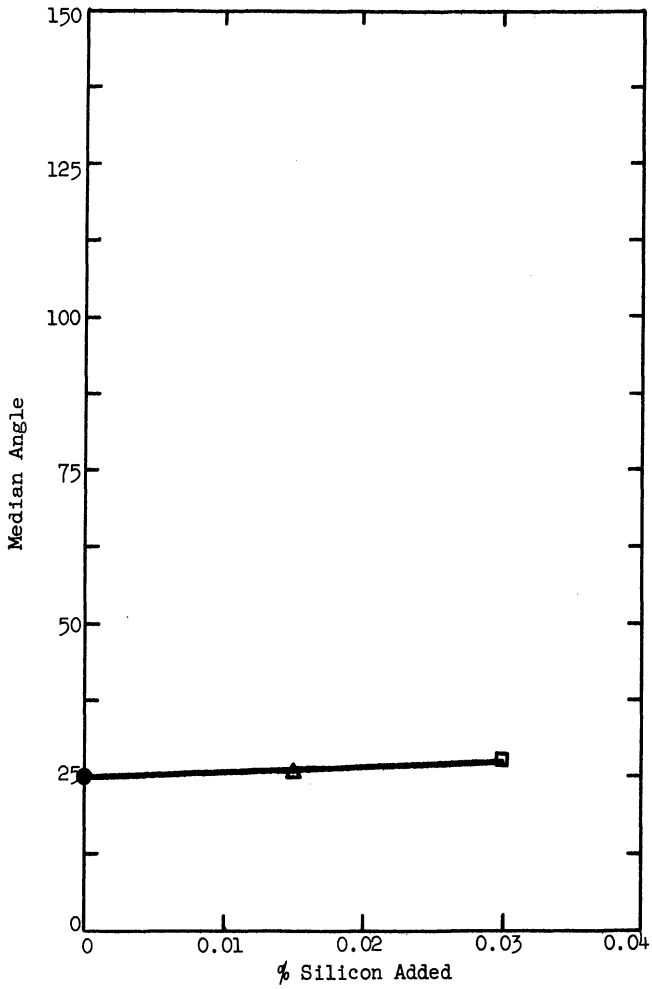

Symbol	Aim Composition, % S	Aim Composition, % Si	Temperature, °F
●	0.30	-----	2300
△	0.30	0.015	2300
□	0.30	0.03	2300

Fig. 3. Effect of silicon.

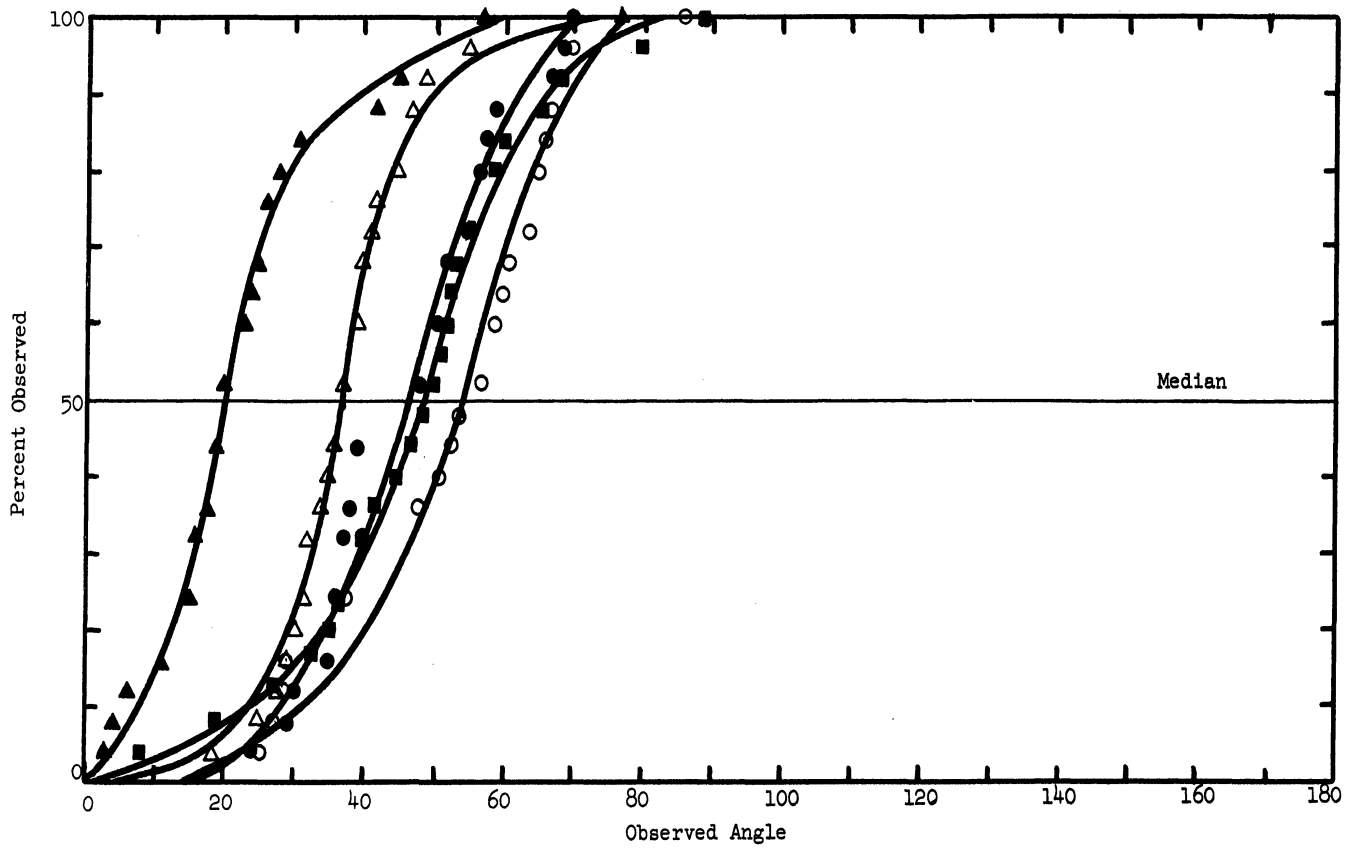

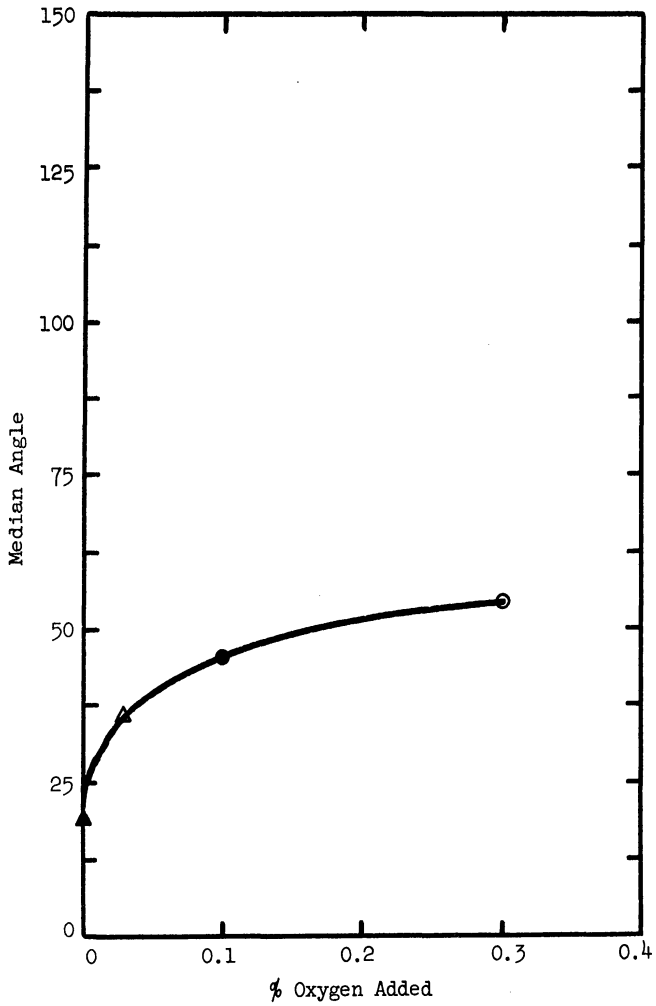

Symbol	Aim Composition, % S	Aim Composition, % O	Temperature, °F
▲	0.30	----	2400
△	0.30	0.03	2400
●	0.30	0.10	2400
○	0.30	0.30	2400
■	0.60	0.60	2400

Fig. 4. Effect of oxygen.

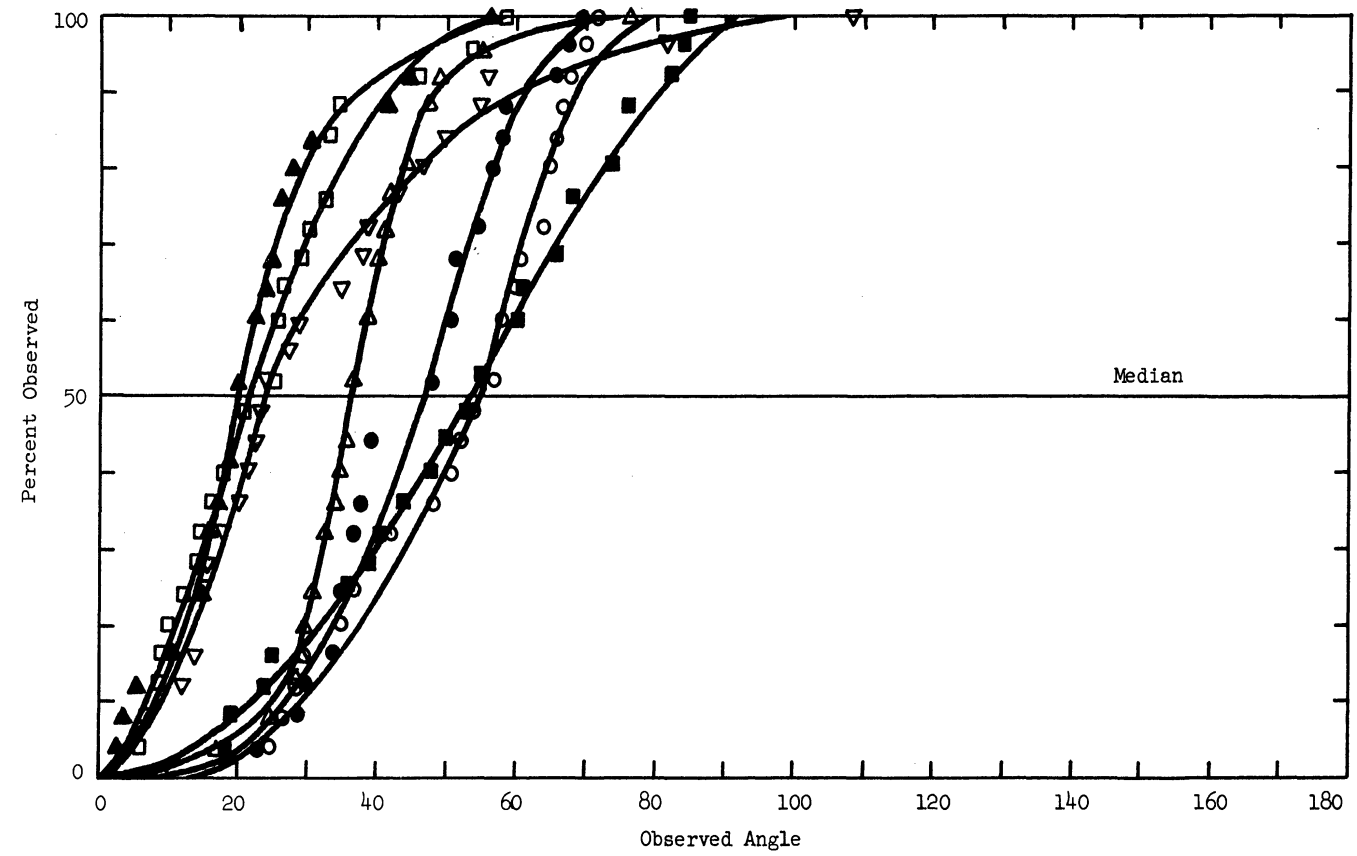

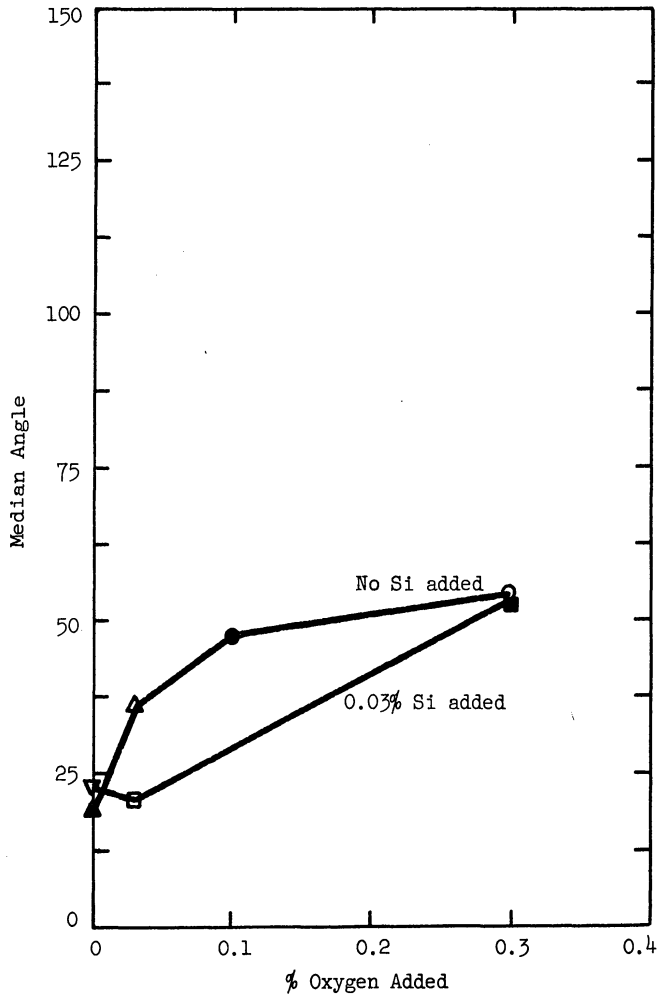

Symbol	Aim Composition, %			Temperature, °F
	S	O	Si	
▲	0.30	----	----	2400
△	0.30	0.03	----	2400
●	0.30	0.10	----	2400
○	0.30	0.30	----	2400
▽	0.30	----	0.03	2400
□	0.30	0.03	0.03	2400
■	0.30	0.30	0.03	2400

Fig. 5. Effect of oxygen and silicon.

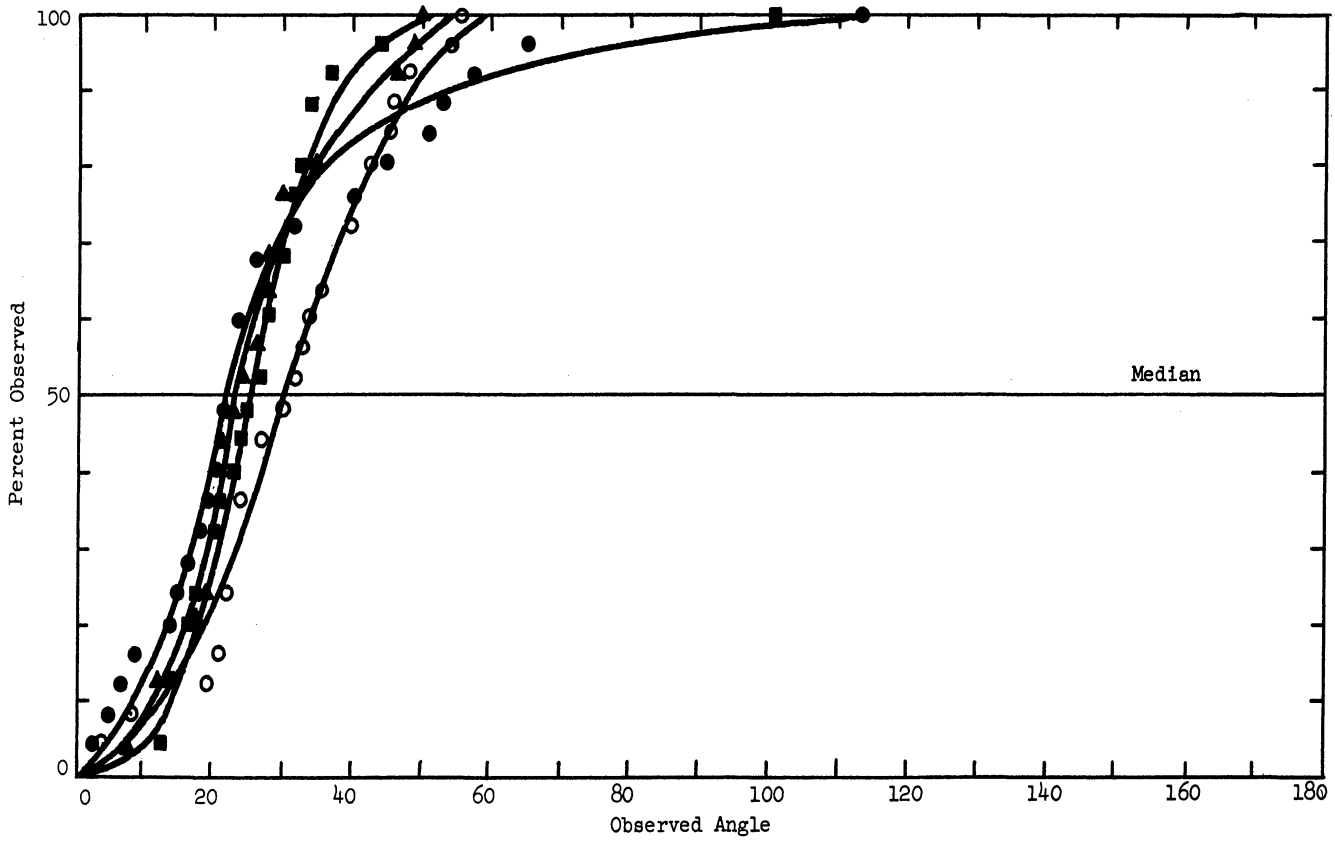

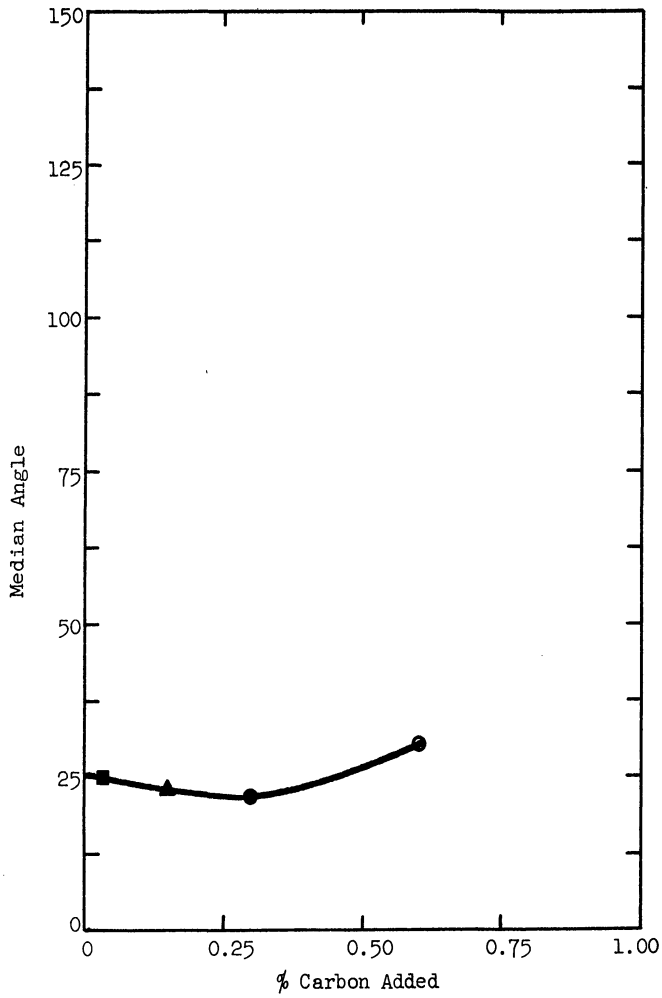

Symbol	Aim Composition, % S	Aim Composition, % C	Temperature, °F
■	0.30	0.03	2300
▲	0.30	0.15	2300
●	0.30	0.30	2300
○	0.30	0.60	2300

Fig. 6. Effect of carbon.

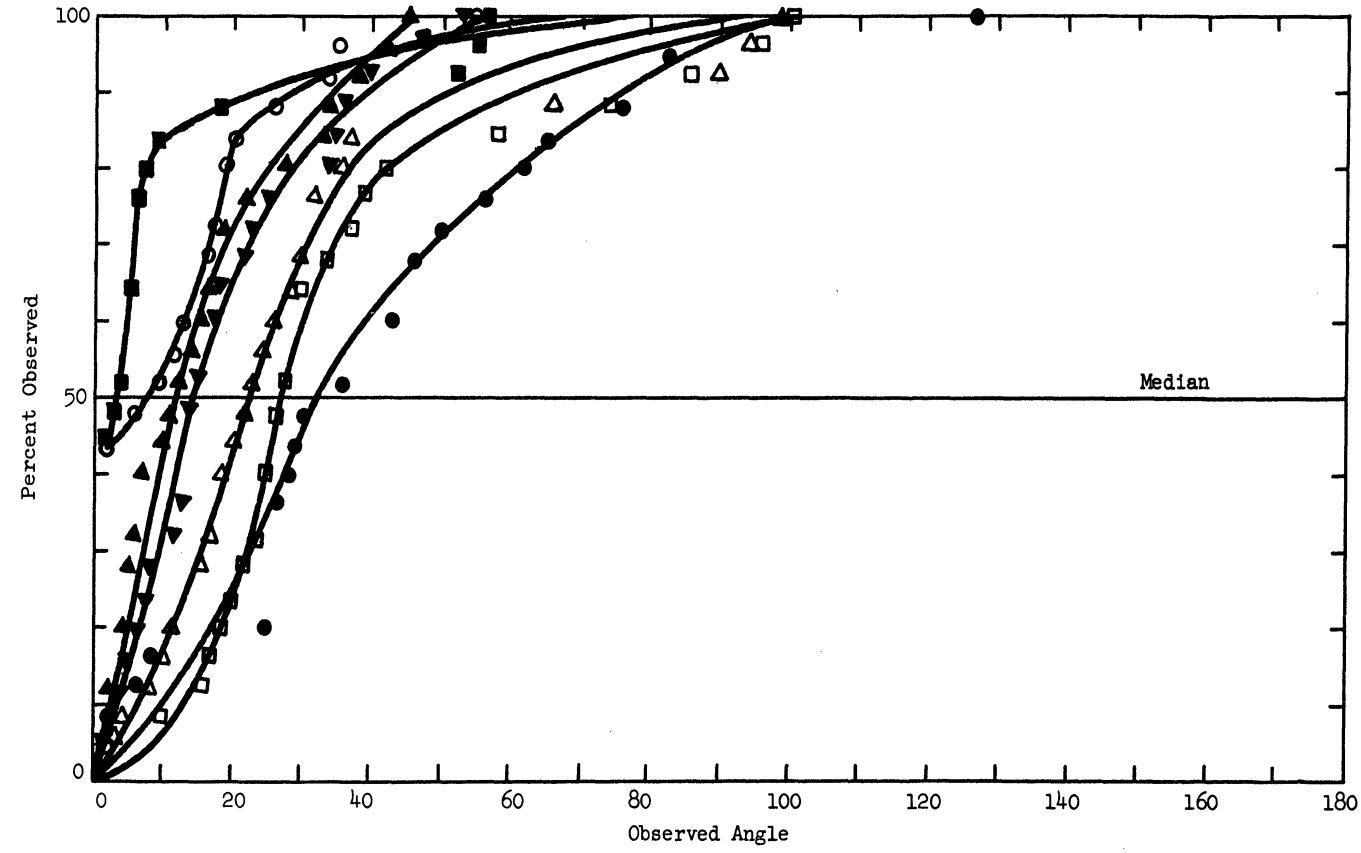

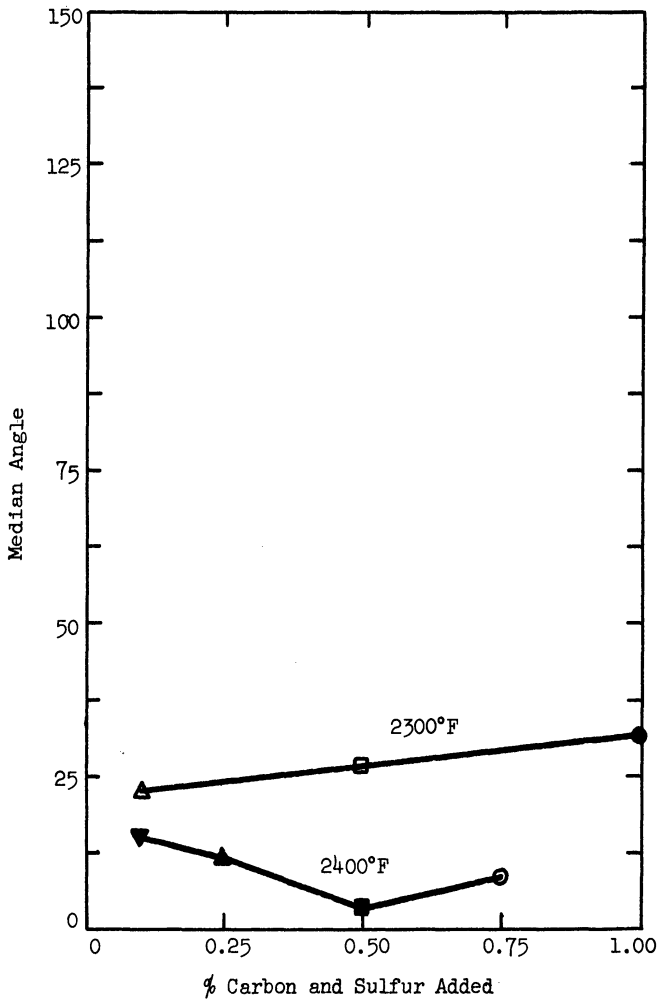

Symbol	Aim Composition, % S	Aim Composition, % C	Temperature, °F
△	0.10	0.10	2300
□	0.50	0.50	2300
●	1.00	1.00	2300
▼	0.10	0.10	2400
▲	0.25	0.25	2400
■	0.50	0.50	2400
○	0.75	0.75	2400

Fig. 7. Effect of carbon and sulfur.

(a) 2300°F X250
(inclusion angle - 27°).

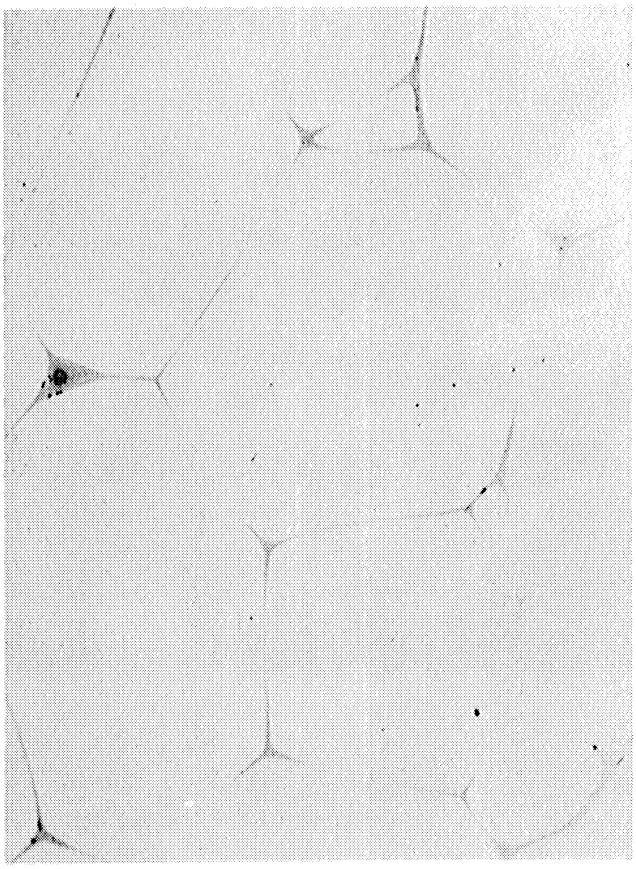

(b) 2400°F X250
(inclusion angle - 8°).

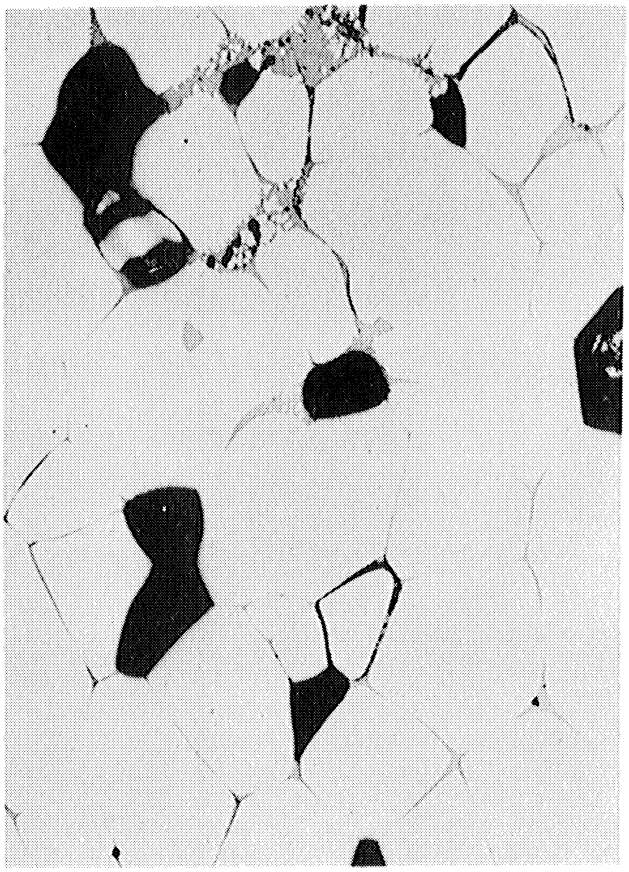

(c) 2400°F X100
(inclusion angle - 8°).

Fig. 8. Intergranular sulfide distribution. In the presence of carbon, the sulfide liquid formed a more complete film at 2400°F (compare Fig. 8b with 1a). A resulting granular embrittlement was observed during polishing by the loss of whole grains. All samples contained additions of 0.5% carbon and 0.5% sulfur.

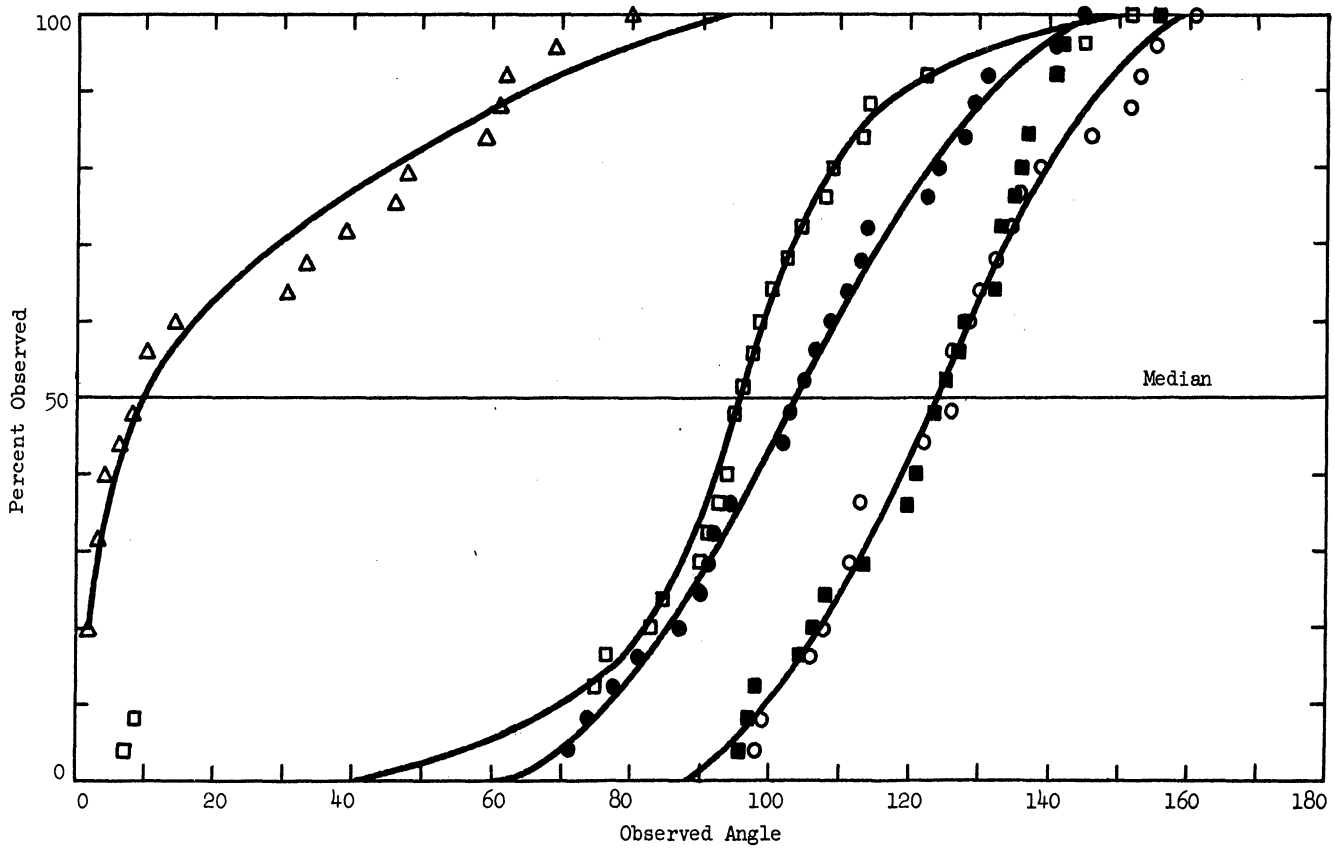

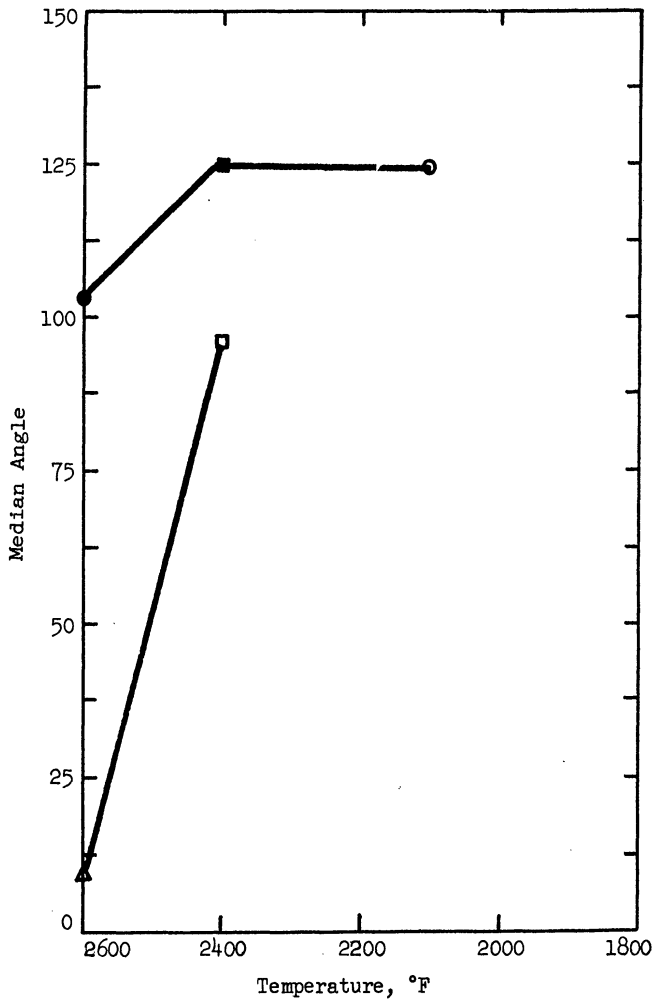

Symbol	Aim Composition, %			Temperature, °F
	S	C	Mn	
●	0.30	0.10	0.90	2600
■	0.30	0.10	0.90	2400
○	0.30	0.10	0.90	2100
△	0.30	0.10	0.15	2600
□	0.30	0.10	0.15	2400

Fig. 9. Effect of manganese.

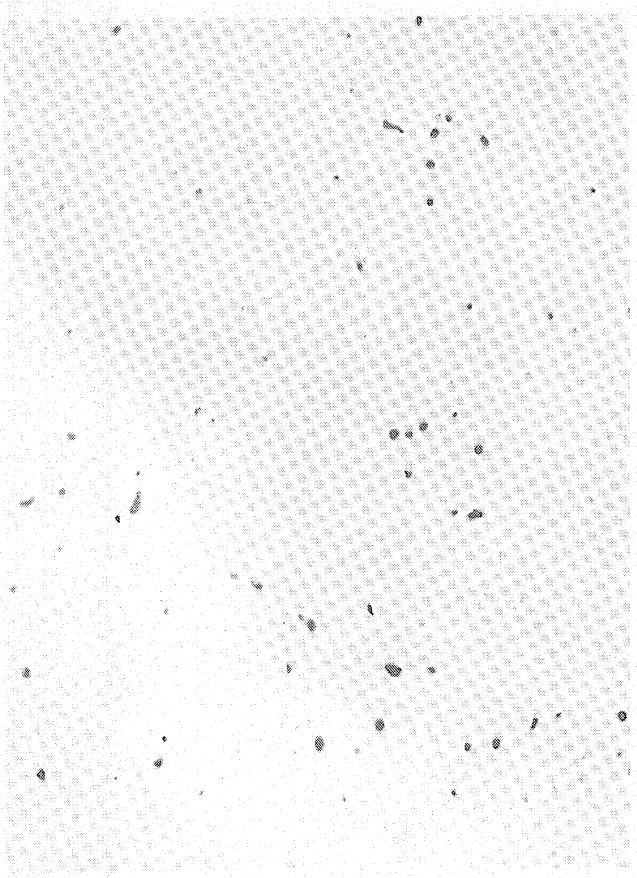

(a) 2400°F 0.9% Mn
(inclusion angle - 124°).

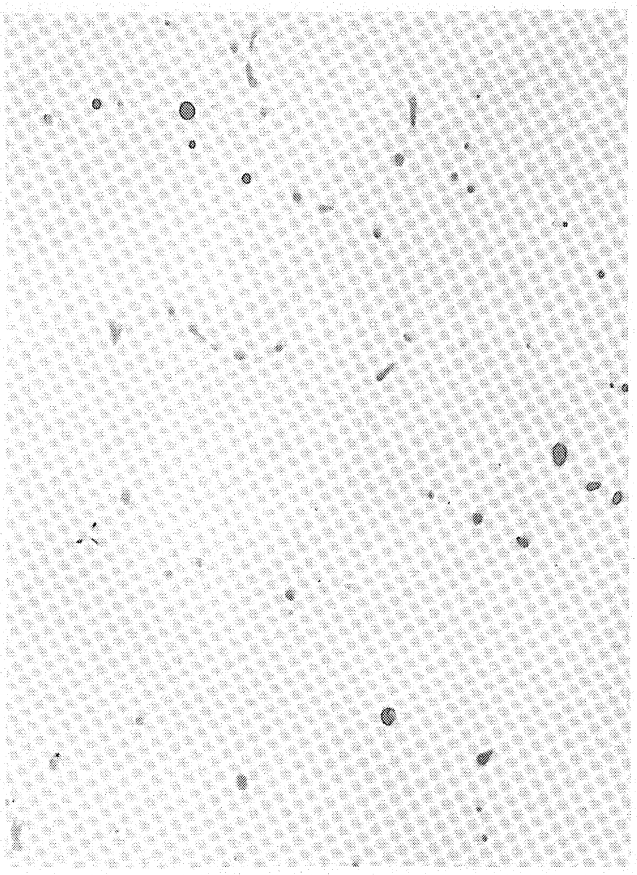

(b) 2600°F 0.9% Mn
(inclusion angle - 104°).

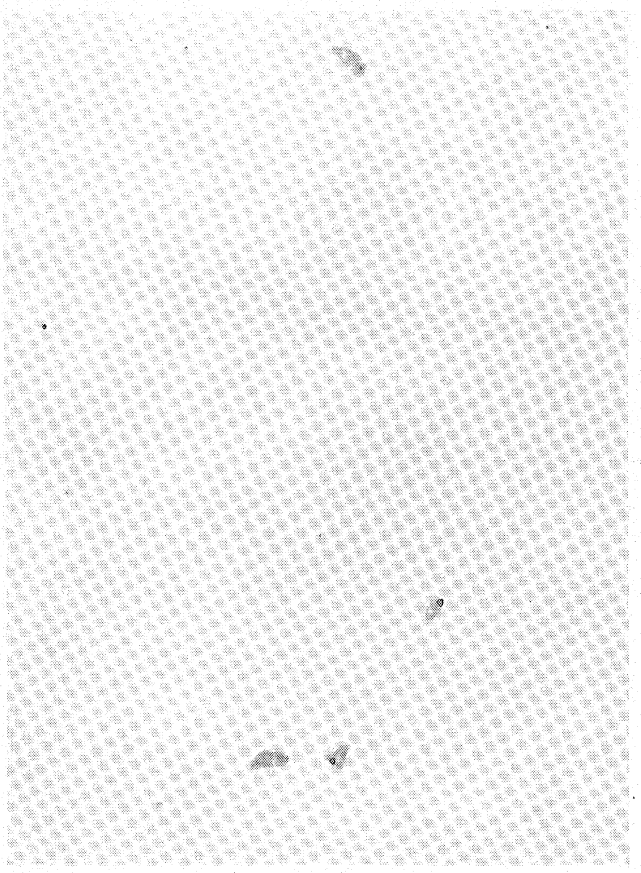

(c) 2400°F 0.15% Mn
(inclusion angle - 96°).

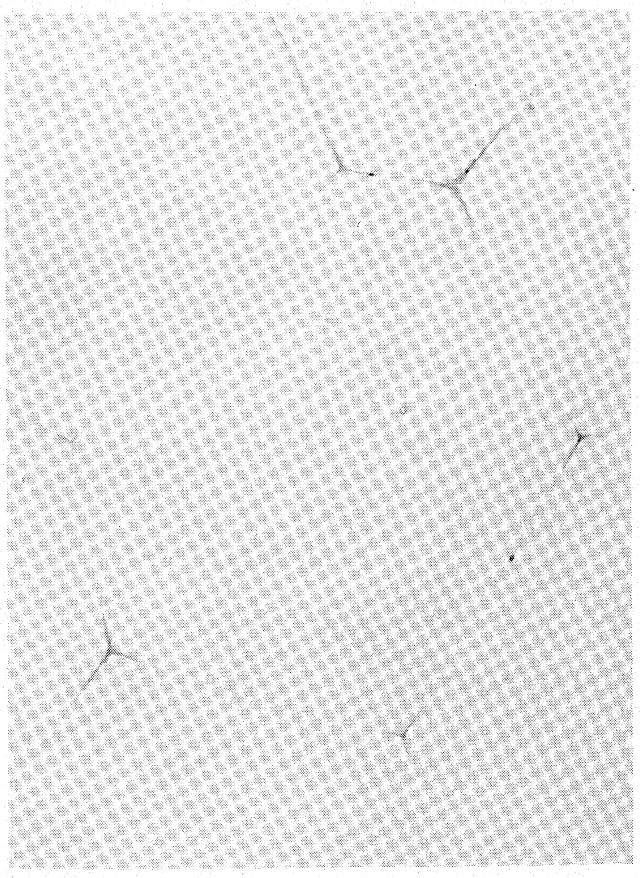

(d) 2600°F 0.15% Mn
(inclusion angle - 10°).

Fig. 10. Effect of manganese on inclusions. X250.

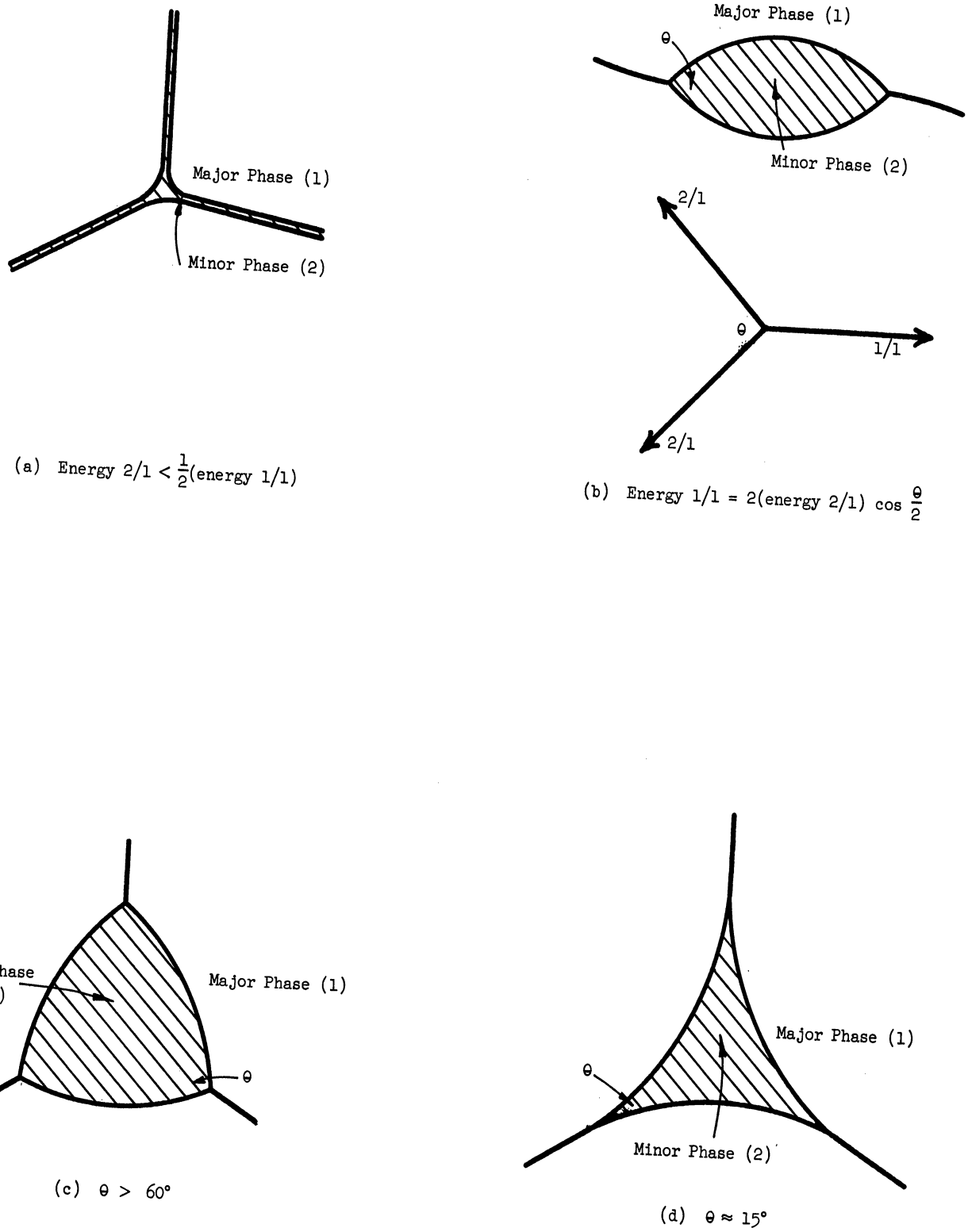

(a) Energy 2/1 < $\frac{1}{2}$(energy 1/1)

(b) Energy 1/1 = 2(energy 2/1) cos $\frac{\theta}{2}$

(c) $\theta > 60°$

(d) $\theta \approx 15°$

Fig. 11. Minor phase distribution.

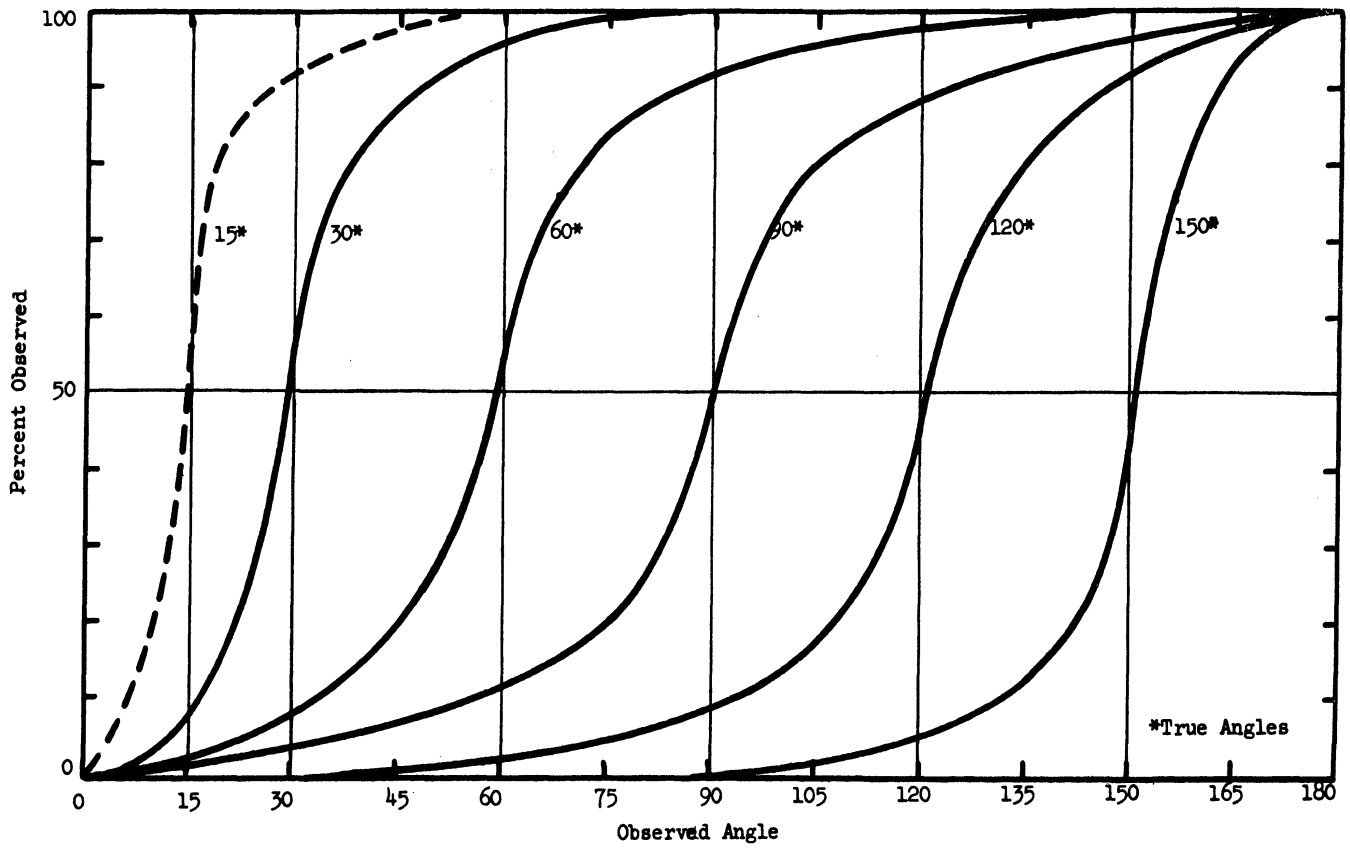

(a) Cumulative curves (theoretical)

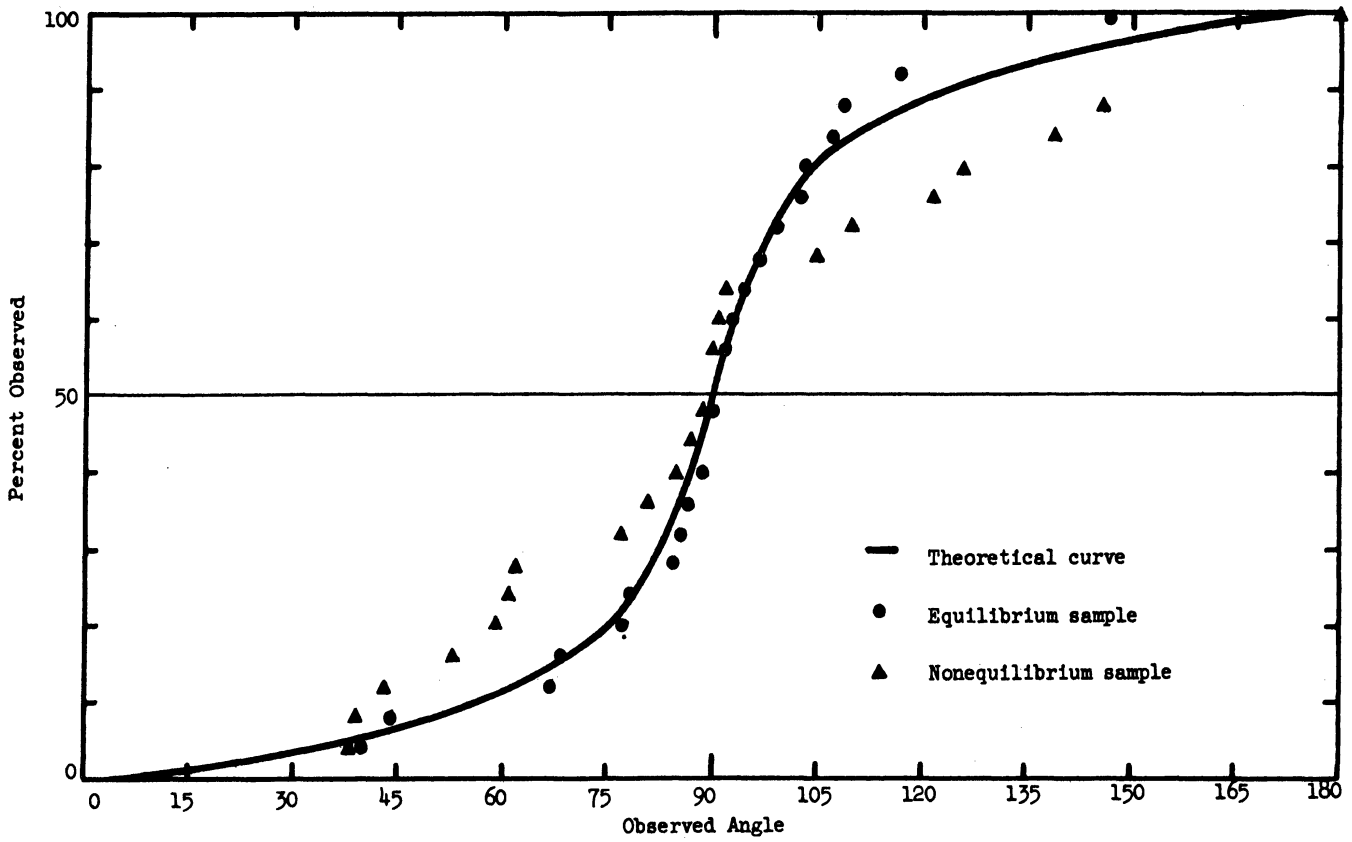

(b) Data Curves

Fig. 12. Shape and distribution indices.

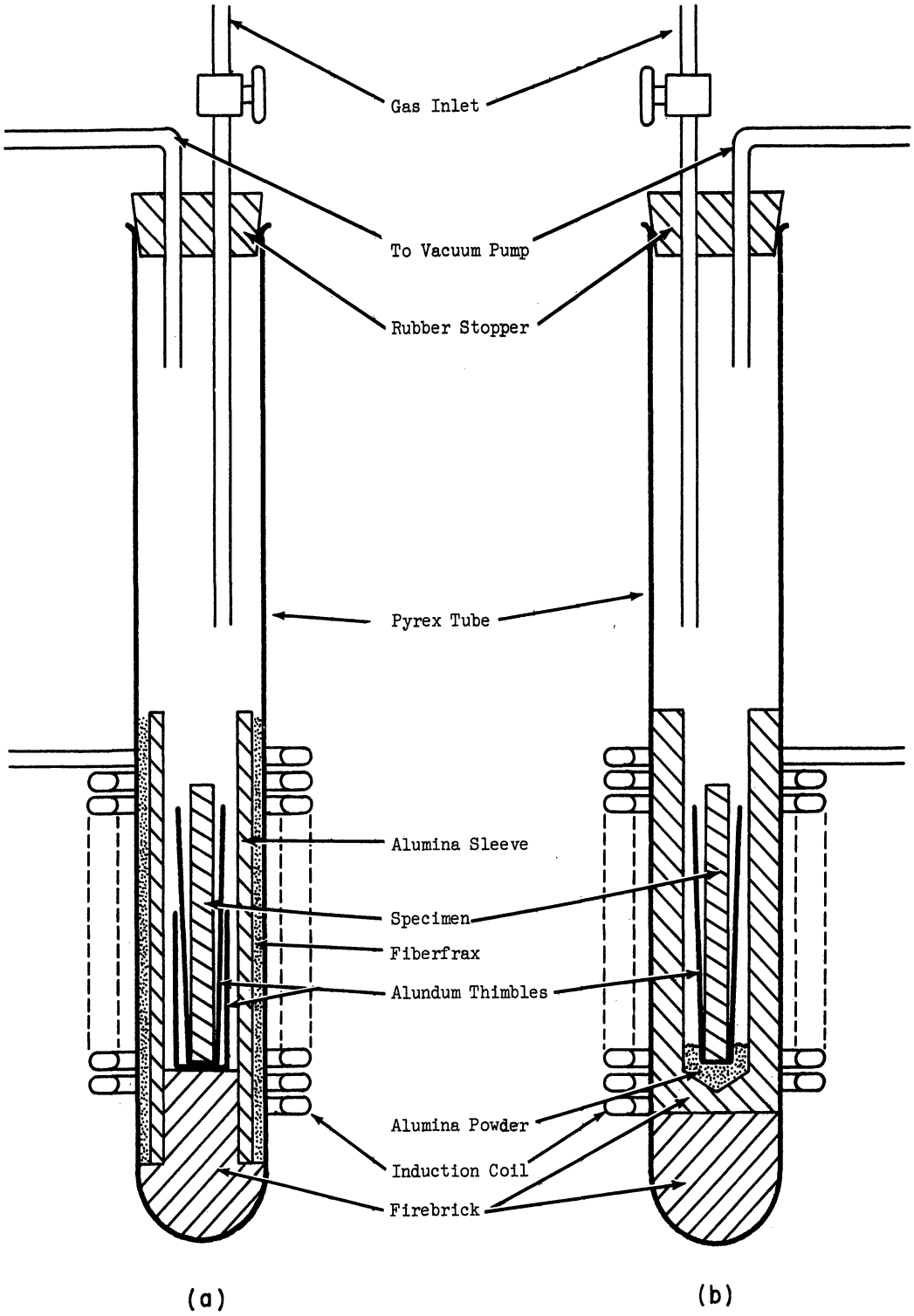

Fig. 13. External coil vacuum-induction furnace.